



## Curvature-adaptive multi-jet polishing of freeform surfaces

Chi Fai Cheung (2), Chunjin Wang, Lai Ting Ho and Jiangbo Chen

Partner State Key Laboratory of Ultraprecision Machining Technology, Department of Industrial and Systems Engineering, The Hong Kong Polytechnic University, Hung Hom, Kowloon, Hong Kong.

This paper presents a curvature-adaptive multi-jet polishing (CAMJP) method that can achieve high efficiency and cater for adaptation of the variation of the material removal rate (*MRR*) to the curvature of freeform surfaces. CAMJP makes use of a purposely designed multi-jet nozzle incorporated with a pressure control system. The effect of surface curvature on the *MRR* is analysed by computational fluid dynamic modelling. The fluid pressure of each jet is controlled independently to vary the *MRR* according to the curvature of freeform surfaces. Experimental results show that CAMJP is effective in improving the accuracy of polishing freeform surfaces.

Polishing, Surface, Multi-jet

### 1. Introduction

Due to the superior functionality of freeform surfaces, they have been widely applied in many fields such as imaging, illumination, aerospace, biomedical engineering, green energy, etc. [1]. Fluid jet polishing (FJP) [2] is one of the promising machining methods for the precision manufacture of freeform surfaces due to its unique advantages such as high machining accuracy, suitability for polishing various kinds of materials, no heat generation during polishing, etc. [3,4]. A multi-jet polishing (MJP) [5] process was proposed to largely enhance the polishing efficiency of FJP, and further extend its applications to medium- to large-sized surfaces.

However, the curvature effect generates considerable residual errors, especially in the FJP of freeform surfaces. Yang, et al. [6] investigated the effect of surface curvature on polishing on an aspheric lens die, and it was found that the polishing area and the central removal depth vary with the surface curvature. Recently, Song, et al. [7] analysed the effect of surface curvature on the polishing parameters in bonnet polishing. Wan, et al. [8] built a tool influence function (*TIF*) model of the small tool polishing process considering the effect of surface curvature. However, research on the effect of surface curvature on the material removal in FJP has received relatively little attention.

To address the problems, this paper first investigates the effect of surface curvature on the material removal characteristics in FJP and a pressure dependent curvature adaptive (PDCA) control method is then proposed to compensate for the error induced by the effect of surface curvature in the MJP of freeform surfaces. Hence, a curvature-adaptive multi-jet polishing (CAMJP) system was established and experiments were conducted to validate its performance in the precision polishing of freeform surfaces.

### 2. Investigation of the effect of surface curvature on the material removal characteristics in FJP

To analyse the effect of surface curvature which refers to the mean curvature [9], the *TIF* on different designed surfaces was determined by a computational fluid dynamic (CFD) model [10] using the FLUENT 17.2 software package. The experiments were divided into five groups according to different impinging angles

(see Table 1). There were concave and convex surfaces with different radii of curvature ( $r$ ). The diameter of the nozzle was 0.5 mm, the stand-off distance was 4 mm, and the polishing slurry was 10 wt. % 1000# silicon carbide (SiC). The workpiece material was S136 mould steel and the fluid pressure of the inlet was 6 bar.

**Table 1**

Surface design for analysing the curvature effect in FJP ('-' signifies convex surface, and '∞' means flat surface)

$\alpha$ (deg)	Radius of curvature $r$ (mm)
90	10,20,30,40,50,75,100, ∞,-100,-75,-50,-40,-30,-20,-10
80	10,20,30,40,50,75,100, ∞,-100,-75,-50,-40,-30,-20,-10
70	10,20,30,40,50,75,100, ∞,-100,-75,-50,-40,-30,-20,-10
60	10,20,30,40,50,75,100, ∞,-100,-75,-50,-40,-30,-20,-10
50	10,20,30,40,50,75,100, ∞,-100,-75,-50,-40,-30,-20,-10

As shown in Figure 1, the material removal rate (*MRR*), which refers to the material volume removal rate of each *TIF*, was determined after simulation.  $\kappa$  is the surface curvature, i.e.

$$\kappa = 1/r \quad (1)$$

It is found that the *MRR* varied from  $4.6 \times 10^{-3}$  mm<sup>3</sup>/min to  $8.2 \times 10^{-3}$  mm<sup>3</sup>/min with various surface curvature and impinging angles. The variation was significant as a critical factor in regard to compensation of the polishing of freeform surfaces.

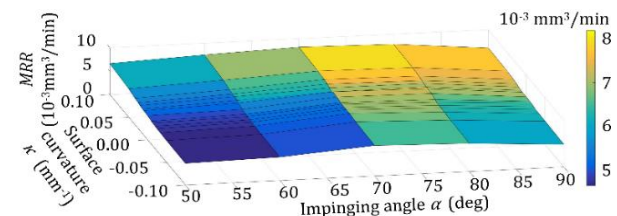


**Figure 1.** Material removal rate in FJP of a workpiece with different surface curvature and impinging angles

To compensate for the variation of *MRR* induced by the variation of the surface curvature and gradient, the relationship among *MRR*, surface curvature and surface gradient was determined first. Besides, a reference *MRR* was needed for comparison. In this study, the *MRR* of the case when the fluid pressure was 6 bar and the impinging angle was 90 degrees, was considered as the

reference *MRR* while other polishing conditions were the same. The *MRR* under different situations divided by the reference *MRR* is defined as the removal rate ratio  $\eta$ . The relationship among  $\eta$ , surface curvature and impinging angle is determined as  $\eta(\alpha, \kappa)$ . Cubic polynomial fitting was used to fit the parametric surface based on the raw data of the *MRR* as deduced from Figure 1, and the fitted surface is shown in Figure 2. The fitted  $\eta_{Fit}(\alpha, \kappa)$  is given below:

$$\begin{aligned} \eta_{Fit}(\alpha, \kappa) &= c_{00} + c_{10}\alpha + c_{01}\kappa + c_{20}\alpha^2 + c_{11}\alpha\kappa + c_{02}\kappa^2 + c_{30}\alpha^3 \\ &+ c_{21}\alpha^2\kappa + c_{12}\alpha\kappa^2 + c_{03}\kappa^3; \\ c_{00} &= 6.505; c_{10} = -0.3043; c_{01} = -0.5136; c_{20} = 0.005321; \\ c_{11} &= 0.1272; c_{02} = 22.44; c_{30} = -0.00002911; \\ c_{21} &= -0.001049; c_{12} = -0.2412; c_{03} = -128.1 \end{aligned} \quad (2)$$

Experiments were conducted on six spherical surfaces specified in Table 2. A comparison between the experimental removal rate ratio  $\eta_{EX}$  and calculated removal rate ratio based on the fitted function  $\eta_{Fit}$  was made. Their difference was less than 10%, which validates the fitted function in Figure 2.

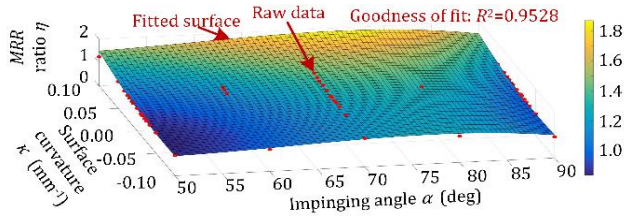


**Figure 2.** *MRR* ratio varies with surface curvature and impinging angle

**Table 2**

Results of the verification of the fitted function  $\eta_{Fit}(\alpha, \kappa)$

$\alpha$ (deg)	$\kappa$ (mm <sup>-1</sup> )	$\eta_{EX}$	$\eta_{Fit}$
70	-1/20	1.233	1.160
77	-1/30	1.338	1.239
80	-1/40	1.364	1.241
82	-1/50	1.285	1.225
83	-1/60	1.259	1.214
85	-1/80	1.175	1.173

### 3. Curvature-adaptive multi-jet polishing method

#### 3.1 Simulation of FJP with and without curvature effect

To further realize the effect of the surface curvature on the material removal characteristics in the FJP of freeform surfaces, a series of simulation experiments was undertaken to simulate the polishing process with and without surface curvature effect. It was assumed that the initial surface form  $H_0(x, y)$  was a F-theta surface with no surface form error, and the size was 20 mm × 40 mm. The polished region was 20 mm × 32 mm, and edge parts were left for reference. The *TIF* was generated by a 0.5 mm diameter nozzle under 6 bar fluid pressure. The material removal depth distribution in a unit time within the *TIF* was defined as the removal function  $R(x, y)$ . A raster tool path with a pitch size of 0.1 mm was adopted in the FJP. The feed rate of 20 mm/min was used, which means that the dwell time  $T(x, y)$  for each dwell point was 0.3 seconds when the distance between them was 0.1 mm. When the target surface is a flat surface corresponding to no surface curvature effect, the distribution of material removal  $E_{Flat}(x, y)$  is derived by Eq. (3) in the discretized form [11],

$$E_{Flat}(x, y) = \sum_i \sum_j R(x - x'_i, y - y'_j) T(x'_i, y'_j) \Delta x'_i \Delta y'_j \quad (3)$$

where  $x'$  and  $y'$  determine the centre position of the removal function during the polishing process. With the effect of the surface curvature of the freeform surface, the distribution of material removal can be expressed as:

$$E_{Freeform}(x, y) = \sum_i \sum_j \eta(x, y) R(x - x'_i, y - y'_j) T(x'_i, y'_j) \Delta x'_i \Delta y'_j \quad (4)$$

where  $\eta(x, y)$  is the removal rate ratio as deduced from  $\eta_{Fit}(\alpha, \kappa)$ . Hence, the final polished surface  $H_{Flat}$  and  $H_{Freeform}$  can be expressed as Eq. (5) and Eq. (6), respectively.

$$H_{Flat} = H_0 - E_{Flat} \quad (5)$$

$$H_{Freeform} = H_0 - E_{Freeform} \quad (6)$$

As shown in Figure 3, the difference between the polished surfaces with and without the surface curvature effect was observed. The difference of the surface form between them was about 0.7  $\mu\text{m}$  when the total removal depth was about 2.4  $\mu\text{m}$ . Hence, the surface curvature should be considered and compensated for in the polishing of freeform surfaces.

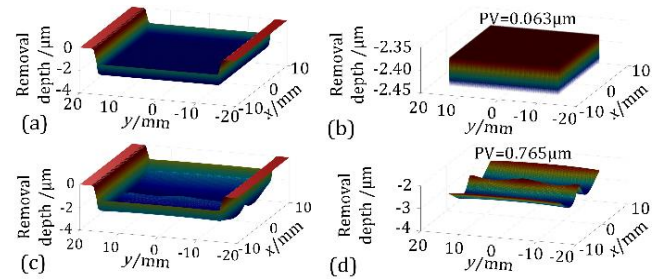


**Figure 3.** Simulation results of the polished surface. (a) Whole surface with no curvature effect, (b) central part of the surface with no curvature effect, (c) whole surface with curvature effect, and (d) central part of the surface with curvature effect (Removed F-theta surface form)

#### 3.2. Pressure-dependent curvature adaptive (PDCA) control method

Since there exists a variation of the *MRR* under different surface curvatures, there is a need to compensate for such variation so as to obtain a high accuracy freeform surface. In fact, the fluid pressure is one of the key factors affecting the *MRR* of FJP [10]. The fluid pressure is real-time controlled by pressure control valves. Hence, the compensation of the effect of curvature variation on *MRR* is accomplished by a real-time control of fluid pressure at different locations of the freeform surfaces.

A pressure-dependent curvature adaptive (PDCA) control method was developed in which the pressure distribution along the polishing path is obtained by the steps: (1) Determine the surface curvature distribution  $\kappa(x, y)$  of the freeform surfaces. (2) Determine the surface gradient distribution of the freeform surface through the calculation of the surface normal vector adopting the function 'surfnorm' in the *MATLAB* software, so as to obtain the impinging angle distribution  $\alpha(x, y)$ . (3) Calculate the distribution of  $\eta$  on the freeform surface based on the fitted function  $\eta_{Fit}(\alpha, \kappa)$ , refer to Eq. (2). (4) Establish the relationship between the fluid pressure  $p$  and  $\eta$ , which is denoted as  $p = f(\eta)$ , where  $\eta$  is calculated in step 3. (5) The fluid pressure distribution is obtained by the function  $p = f(\eta)$  and the tool path information, where  $\eta = \eta(\alpha, \kappa)$ . As mentioned in step 4, the relationship between  $p$  and  $\eta$  is established through experiments.  $p$  varied from 3 bar to 8 bar. The dwell time for each *TIF* was 2 minutes. Other conditions were the same as the simulation conditions. Figure 4(a) shows the relationships between  $p$  and *MRR*. The deduced relationship between the required  $p$  and  $\eta$  is shown in Figure 4(b).

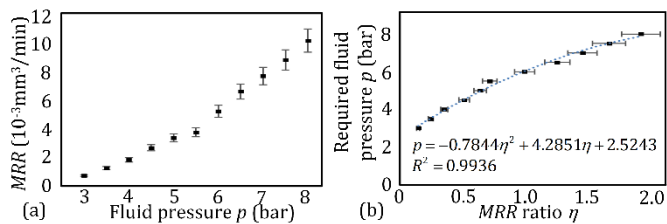


**Figure 4.** Experimental results of the relationships: (a)  $MRR$  varies with pressure, and (b) required fluid pressure varies with  $MRR$  ratio

### 3.3. The curvature adaptive multi-jet polishing system

Based on the PDCA control method, a curvature-adaptive multi-jet polishing (CAMJP) system was built by incorporating an array of pressure control valves and corresponding control unit into the traditional MJP system [5] (see Figure 5). In the CAMJP system, each fluid jet is operated independently to maintain stable control of the material removal during polishing. Since there exists fluid flow interference [5], a suitable jet distance was determined. The CFD modelling and simulation was used to study the effect of jet distance on the material removal characteristics. Two fluid jets with a 0.5 mm diameter orifice and four different jet distances were designed based on the simulation results (see Figure 6).

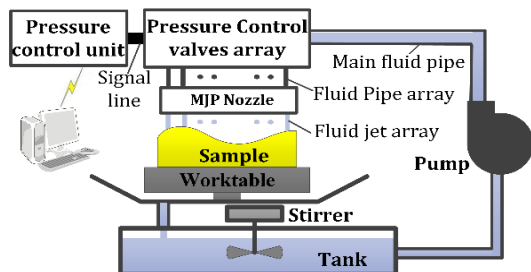


**Figure 5.** Schematic diagram of the CAMJP system

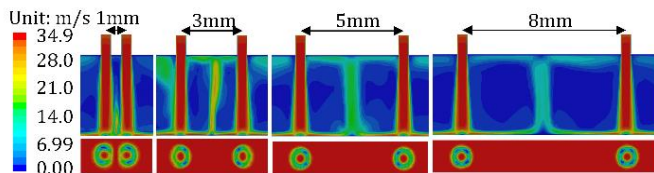


**Figure 6.** Simulated fluid velocity distribution and corresponding material removal depth contour under different fluid jet distances

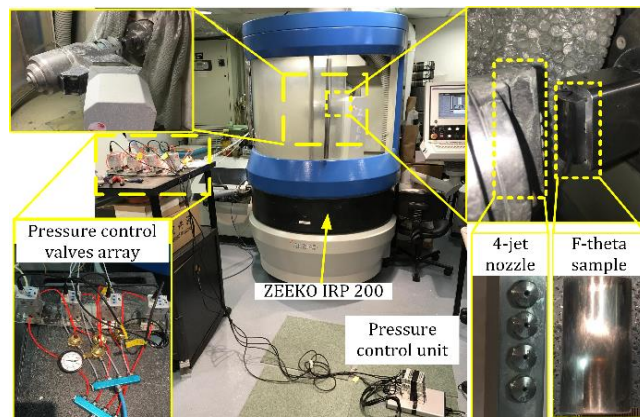
The shape of the material removal footprint generated by each jet was highly distorted when the jet distance was small. With increasing jet distance, the footprint shape became axisymmetric. When the fluid jet distance was 8 mm, the flow jet interference became very small, as reflected in the flow velocity of the up flow at the centre. Moreover, two generated footprints were similar in shape as generated by single jet polishing. As a result, a 0.5 mm diameter orifice with an 8 mm jet distance was adopted. A multi-jet nozzle integrated with four linearly distributed orifices was purposely designed for implementation of the CAMJP system.

## 4. Experimental verification

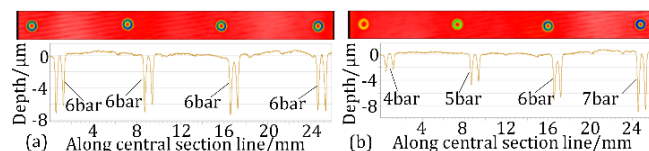
### 4.1. Characterization of tool influence function

Figure 7 shows the experimental setup of the CAMJP system which was built based on a ZEEKO IRP200 polishing machine. The designed 4-jet nozzle was assembled on the spindle of the machine, and the pressure of each jet was controlled by four independent fluid pressure control valves. The orifice diameter was 0.5 mm and the distance between each orifice was 8 mm. The orifice was made of sapphire to avoid tool wear. The pressure control unit USB6343

from National Instruments in the USA was used to control the pressure. To evaluate the performance of the CAMJP system, the  $TIF$  of the MJP tool was tested on flat S136 mould steel. The polishing slurry was 10 wt. % 1000# SiC. Two  $TIF$ s were used including one with four uniform fluid pressures and the other with four different fluid pressures (see Figure 8). Figure 8(a) shows that the  $TIF$  of each jet had high uniformity and the effect of the jet interference was not found. Figure 8(b) shows the effective control of the  $MRR$  by the fluid pressure.



**Figure 7.** Configuration of the experimental setup for CAMJP



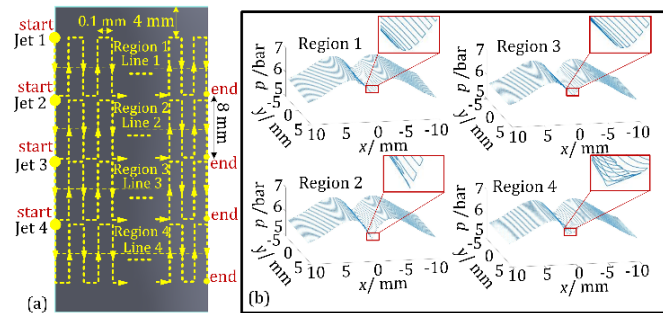
**Figure 8.** Measured tool influence function of the 4-jet multi-jet polishing tool (a) under the same pressure, and (b) different pressure

### 4.2. Curvature adaptive multi-jet polishing of freeform surfaces

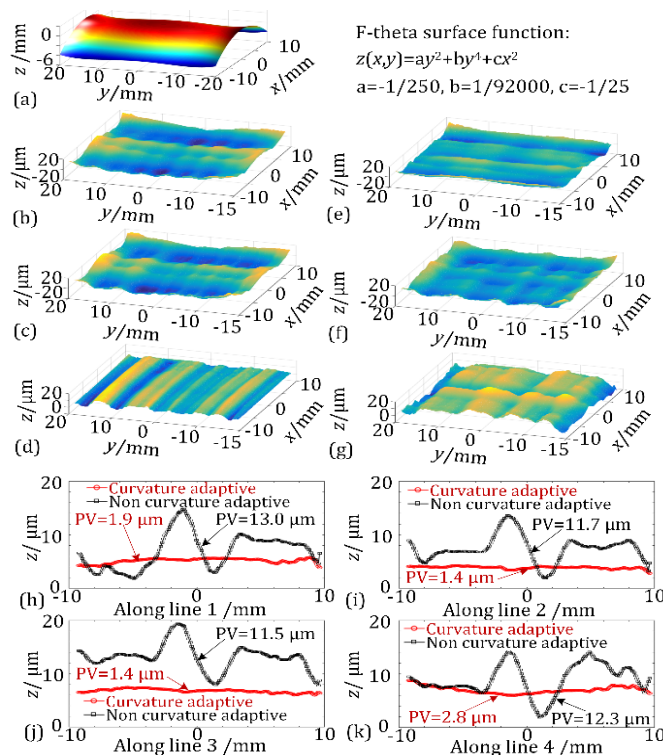
To evaluate the performance of the CAMJP system, polishing experiments were conducted on freeform surfaces. The workpiece was a 20 mm  $\times$  40 mm S136 mould steel F-theta lens surface. The form error of the workpiece before and after polishing was measured by a Werth Video Check UA Coordinate measuring machine. Experiments were conducted on two F-theta lens samples with one polished by CAMJP, while the other was polished by traditional MJP without pressure compensation. Figure 9(a) shows the raster tool path with a pitch size of 0.1 mm. The top and bottom edges with a length of 4 mm remain for reference. Each jet is only needed to move in each sub-region while it needs to move in the whole region for traditional single jet polishing. In the traditional MJP, the fluid pressure was kept at 6 bar. Figure 9(b) shows the fluid pressure distribution of each jet in CAMJP, which was determined by the method mentioned in section 3.2. Both feed rates were 20 mm/min. Two polishing cycles were applied for each sample.

Figure 10(a) shows the F-theta surface form and its surface function. The surface form error of sample 1 before and after CAMJP is shown in Figure 10(b) and Figure 10(c), while Figure 10(e) and Figure 10(f) shows the surface form error of sample 2 before and after traditional MJP. The surface form of the workpiece before and after polishing was registered and extracted by the iterative closest point algorithm [12] so as to obtain the material removal distribution (see Figure 10(d) and Figure 10(g)). The distribution of material removal after CAMJP was found to be more uniform than that for traditional MJP, which validates the effectiveness of CAMJP. The distribution of material removal of four independent regions was analysed through extracting the data along the four sectional lines as shown in Figure 10(h) to

Figure 10(k). The distribution of material removal in CAMJP was found to be much more uniform than that for traditional MJP, which is reflected by the peak-to-valley (PV) value of the material removal curve. This infers that the PDCA control method is effective for compensating the variation of material removal due to variation of surface curvature and the CAMJP system can improve the form error in the polishing of freeform surfaces.



**Figure 9.** Tool path planning for (a) each jet on the F-theta surface and (b) pressure distribution along the tool path for curvature-adaptive polishing



**Figure 10.** Comparison of polished surface form between CAMJP and traditional MJP. (a) F-theta surface form and function, surface form error of sample 1 (b) before CAMJP and (c) after CAMJP, (d) material removal of sample 1, surface form error of sample 2 (e) before and (f) after traditional MJP, (g) material removal of sample 2, comparison of the material removal along (h) line 1, (i) line 2, (j) line 3 and (k) line 4 as shown in Figure 9(a)

Figure 11(a) and Figure 11(b) shows the F-theta surface before and after CAMJP. The surface roughness of the workpiece was measured by a Zygo NexView optical profiler at five different positions on the polished surface. The arithmetic roughness ( $R_a$ ) of the F-theta surface after traditional MJP was improved from 211 nm to 30 nm, while the  $R_a$  value after CAMJP was improved from 215.7 nm to 23.7 nm. Another two polishing experiments adopting CAMJP were conducted on two F-theta surfaces with different initial roughness. As shown in Figure 11(c), the surface finish after CAMJP was as good as after traditional MJP. This is attributed to the same material removal mechanism. Although the PDCA method may add to the complexity of the system, it can be

implemented by people with state-of-the-art skills. More importantly, it provides a compensation solution for the form error caused by the surface curvature effect in FJP and MJP.

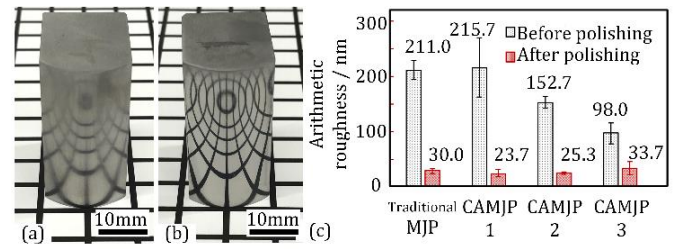


**Figure 11.** Snapshots of F-theta surface (a) before and (b) after CAMJP, (c) measured arithmetic roughness of samples before and after polishing

## 5. Conclusions

In this study, the effect of surface curvature on the material removal in fluid jet polishing (FJP) of freeform surfaces was analysed by computational fluid dynamic modelling. The results show that the material removal rate ( $MRR$ ) varies with the surface curvature in FJP of freeform surfaces. A pressure-dependent curvature adaptive (PDCA) control method was innovatively developed to control the pressure for each jet of the multi-jet nozzle so as to compensate for the variation of  $MRR$  due to the variation of surface curvature in the polishing of freeform surfaces. Hence, a novel curvature-adaptive multi-jet polishing (CAMJP) system was built based on the PDCA control method with a purposely designed multi-jet nozzle. Experimental results show that the PDCA control method is effective and the CAMJP system can achieve high form accuracy and good surface finish in the polishing of freeform surfaces.

## Acknowledgements

The authors would like to express their sincere thanks for the financial support from the Research Office (Project code: BBX7).

## References

- [1] Fang FZ, Zhang XD, Weckenmann A, Zhang GX, Evans C (2013) Manufacturing and Measurement of Freeform Optics. *CIRP Annals-Manufacturing Technology* 62(2):823-846.
- [2] Föhnle OW, Van Brug H, Frankena HJ (1998) Fluid Jet Polishing of Optical Surfaces. *Applied Optics* 37(28):6771-6773.
- [3] Beaucamp A, Namba Y, Freeman R (2012) Dynamic Multiphase Modeling and Optimization of Fluid Jet Polishing Process. *CIRP Annals-Manufacturing Technology* 61(1): 315-318.
- [4] Beaucamp A, Namba Y (2013) Super-Smooth Finishing of Diamond Turned Hard X-Ray Molding Dies by Combined Fluid Jet and Bonnet Polishing. *CIRP Annals-Manufacturing Technology* 62(1): 315-318.
- [5] Wang CJ, Cheung CF, Ho LT, Liu MY, Lee WB (2017) A Novel Multi-jet Polishing Process and Tool for High-Efficiency Polishing. *International Journal of Machine Tools and Manufacture* 115:60-73.
- [6] Yang MY, Lee HC (2001) Local Material Removal Mechanism Considering Curvature Effect in the Polishing Process of the Small Aspherical Lens Die. *Journal of Materials Processing Technology* 116(2):298-304.
- [7] Song J, Yao Y, Dong Y, Dong B (2017) Prediction of Surface Quality considering the Influence of The Curvature Radius for Polishing of a Free-Form Surface based on Local Shapes. *The International Journal of Advanced Manufacturing Technology* 1-15.
- [8] Wan S, Zhang X, Zhang H, Xu M, Jiang X (2017) Modeling and Analysis of Sub-aperture Tool Influence Functions for Polishing Curved Surfaces. *Precision Engineering* 51:415-425.
- [9] Goldman R (2005) Curvature Formulas for Implicit Curves and Surfaces. *Computer Aided Geometric Design* 22(7):632-658.
- [10] Wang CJ, Cheung CF, Liu MY (2017) Numerical Modelling and Experimentation of Three Dimensional Material Removal Characteristics in Fluid Jet Polishing. *International Journal of Mechanical Sciences* 133:568-577.
- [11] Wang C, Yang W, Wang Z, Yang X, Hu C, Zhong B, Guo Y, Xu Q (2014) Dwell-Time Algorithm for Polishing Large Optics. *Applied Optics* 53(21):4752-4760.
- [12] Besl, PJ, McKay, ND (1992) A method for registration of 3-D shapes. *IEEE Transactions on Pattern Analysis and Machine Intelligence* 14(2):239-256.